

# 6 / Film Deposition

Fabrication processes involve many steps in which thin films of various materials are deposited on the surface of the wafer. This chapter presents a survey of deposition processes, including evaporation, chemical vapor deposition, and sputtering, which are used to deposit metals, silicon and polysilicon, and dielectrics such as silicon dioxide and silicon nitride. Evaporation and sputtering require vacuum systems operating at low pressure, whereas chemical vapor deposition and epitaxy can be performed at either reduced or atmospheric pressure. An overview of vacuum systems and some *results from* the theory of ideal gases are also presented in this chapter.

## 6.1 EVAPORATION

Physical evaporation is one of the oldest methods of depositing metal films. Aluminum and gold are heated to the point of vaporization, and then evaporate to form a thin film covering the surface of the silicon wafer. In order to control the composition of the deposited material, evaporation is performed under vacuum conditions.

Figure 6.1 shows a basic vacuum deposition system consisting of a vacuum chamber, a mechanical roughing pump, a diffusion pump or turbomolecular pump, valves, vacuum gauges, and other instrumentation. In operation, the roughing valve is opened first, and the mechanical pump lowers the vacuum chamber pressure to an intermediate vacuum level of approximately 1 Pascal ( $\text{Pa}^1$ ). If a higher vacuum level is needed, the roughing valve is closed, and the foreline and high-vacuum valves are opened. The roughing pump now maintains a vacuum on the output of the diffusion pump. A liquid-nitrogen (77 K) cold trap is used with the diffusion pump to reduce the pressure in the vacuum chamber to approximately  $10^{-4}$  Pa. Ion and thermocouple gauges are used to monitor the pressure at a number of points in the vacuum system, and several other valves are used as vents to return the system to atmospheric pressure.

---

<sup>1</sup> 1 atm = 760 mm Hg = 760 torr =  $1.013 \times 10^5$  Pa. 1 Pa = 1 N/m<sup>2</sup> = 0.0075 torr.

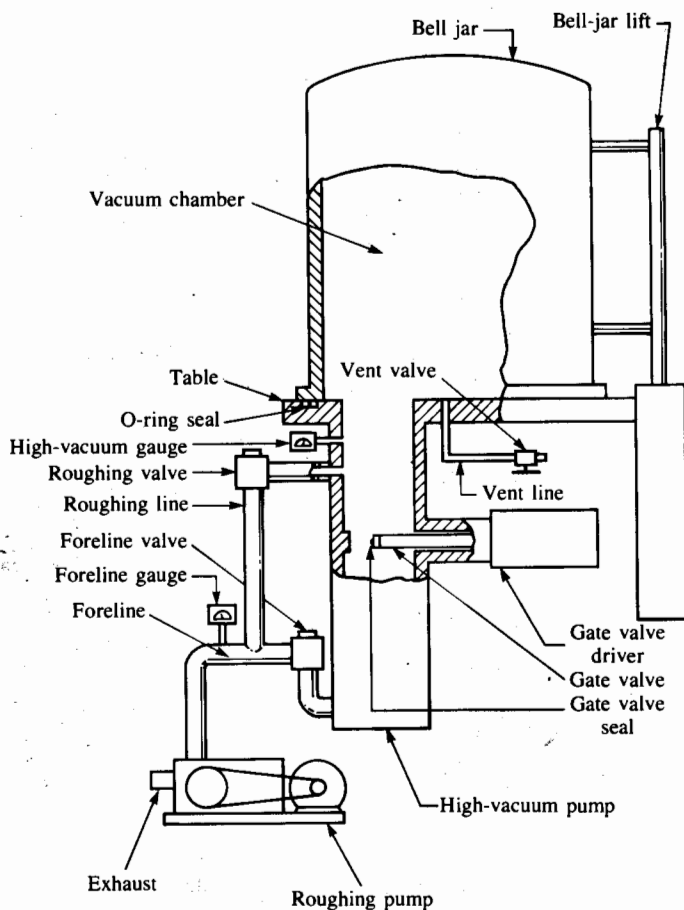


**Fig. 6.1** Typical vacuum system used for evaporation including vacuum chamber, roughing pump, high-vacuum pump, and various valves and vacuum gauges. Copyright, 1987, McGraw-Hill Book Company; reprinted with permission from ref. [5].

### 6.1.1 Kinetic Gas Theory

Gases behave in an almost ideal manner at low pressure and are well described by the ideal gas law. Pressure  $P$ , volume  $V$ , and temperature  $T$  of one mole of a gas are related by

$$PV = N_{av}kT \quad (6.1)$$

in which  $k^\dagger$  is Boltzmann's constant and  $N_{av}$  is Avogadro's number ( $6.02 \times 10^{23}$

<sup>†</sup>  $k$  (Boltzmann's constant) =  $1.38 \times 10^{-23}$  J/K =  $1.37 \times 10^{-22}$  atm-cm<sup>3</sup>/K.

molecules/mole). The concentration of gas molecules is given by

$$n = N_{av}/V = [kT/P]^{-1} \quad (6.2)$$

In some systems, the surface of the substrate must be kept extremely clean prior to deposition. The presence of even a small amount of oxygen or other elements will result in formation of a contamination layer on the surface of the substrate. The rate of formation of this layer is determined from the impingement rate of gas molecules hitting the substrate surface and is related to the pressure by

$$\Phi = P/\sqrt{2\pi mkT} \text{ (molecules/cm}^2\text{-sec)} \quad (6.3)$$

where  $m$  is the mass of the molecule. This can be reduced to

$$\Phi = 2.63 \times 10^{20} P/\sqrt{MT} \text{ (molecules/cm}^2\text{-sec)} \quad (6.4)$$

where  $P$  is the pressure in Pa and  $M$  is the molecular weight (e.g.,  $M = 32$  for oxygen molecules). If we assume that each molecule sticks as it contacts the surface, then the time required to form a monolayer on the surface is given by

$$t = N_s/\Phi = N_s\sqrt{2\pi mkT}/P \quad (6.5)$$

where  $N_s$  is the number of molecules/cm<sup>2</sup> in the layer.

**Example:** Suppose the residual pressure of oxygen in the vacuum system is 1 Pa. How long does it take to deposit one atomic layer of oxygen on the surface of the wafer at 300 K?

**Solution:** The radius of an oxygen molecule is approximately 3.6 Å. If we assume close packing of the molecules on the surface, there will be approximately  $2.2 \times 10^{14}$  molecules/cm<sup>2</sup>. At 300 K and 1 Pa, the impingement rate for oxygen is  $2.7 \times 10^{18}$  molecules/cm<sup>2</sup>-sec. One monolayer is deposited in 82 μsec.

Pressure and temperature also determine another important film-deposition parameter called the *mean free path*,  $\lambda$ . The mean free path of a gas molecule is the average distance the molecule travels before it collides with another molecule.  $\lambda$  is given by

$$\lambda = kT/\sqrt{2} \pi P d^2 \quad (6.6)$$

in which  $d$  is the diameter of the gas molecule and is in the range of 2 to 5 Å. Evaporation is usually done at a background pressure near  $10^{-4}$  Pa. At this pressure, a 4-Å molecule has a mean free path of approximately 60 m. Thus, during aluminum evaporation, for example, aluminum molecules do not interact with the background gases and tend to travel in a straight line from the evaporation source to the deposition target.

On the other hand, sputtering, which will be discussed in Section 6.4, uses argon gas at a pressure of approximately 100 Pa. Using the same radius results in a mean free path of only 60  $\mu\text{m}$ . Thus the material being deposited tends to scatter often with the argon atoms and arrives at the target from random directions.

### 6.1.2 Filament Evaporation

The simplest evaporator consists of a vacuum system containing a filament which can be heated to high temperature. In Fig. 6.2a, small loops of a metal such as aluminum are hung from a filament formed of a refractory (high-temperature) metal such as tungsten. Evaporation is accomplished by gradually increasing the temperature of the filament until the aluminum melts and wets the filament. Filament temperature is then raised to evaporate the aluminum from the filament. The wafers are mounted near the filament and are covered by a thin film of the evaporating material.

Although filament evaporation systems are easy to set up, contamination levels can be high, particularly from the filament material. In addition, evaporation of composite materials cannot be easily controlled using a filament evaporator. The material with the lowest melting point tends to evaporate first, and the deposited film will not have the

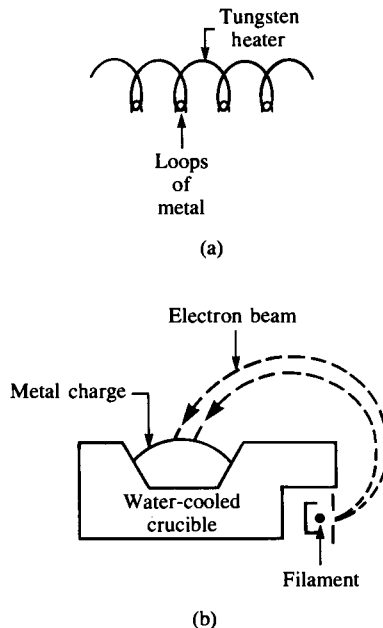


**Fig. 6.2** Two forms of evaporation sources. (a) Filament evaporation, in which loops of wire hang from a heated filament; (b) electron-beam source in which a beam of electrons is focused on a metal charge. The beam is bent in a magnetic field.

same composition as the source material. Thick films are difficult to achieve since a limited supply of material is contained in the metal loops.

### 6.1.3 Electron-Beam Evaporation

In electron-beam (E-beam) evaporation systems (see Fig. 6.2b), the high-temperature filament is replaced with an electron beam. A high-intensity beam of electrons, with an energy up to 15 keV, is focused on a source target containing the material to be evaporated. The energy from the electron beam melts a region of the target. Material evaporates from the source and covers the silicon wafers with a thin layer.

The growth rate using a small planar source is given by

$$G = \frac{m}{\pi \rho r^2} \cos \phi \cos \theta \text{ (cm/sec)} \quad (6.7)$$

for the geometrical setup in Fig. 6.3.  $\phi$  is the angle measured from the normal to the plane of the source, and  $\theta$  is the angle of the substrate relative to the vapor stream.  $\rho$  and  $m$  are the density ( $\text{g/cm}^3$ ) and mass evaporation rate ( $\text{g/sec}$ ), respectively, of the material being deposited.

For batch deposition, a planetary substrate holder (Fig. 6.4) consisting of rotating sections of a sphere is used. Each substrate is positioned tangential to the surface of the sphere with radius  $r_0$ , as in Fig. 6.3. Application of some geometry yields

$$\cos \theta = \cos \phi = r/2r_0 \quad (6.8)$$

For the planetary substrate holder,  $G$  becomes independent of substrate position:

$$G = m/4\pi \rho r_0^2 \quad (6.9)$$

The wafers are mounted above the source and are typically rotated around the source during deposition to ensure uniform coverage. The wafers are also often radiantly heated to improve adhesion and uniformity of the evaporated material. The source material sits in a water-cooled crucible, and its surface only comes in contact with the electron beam during the evaporation process. Purity is controlled by the purity of the original source material. The relatively large size of the source provides a virtually unlimited supply of material for evaporation, and the deposition rate is easily controlled by changing the current and energy of the electron beam.

One method of monitoring the deposition rate uses a quartz crystal which is covered by the evaporating material during deposition. The resonant frequency of the crystal shifts in proportion to the thickness of the deposited film. By monitoring the resonant frequency of the crystal, the deposition rate may be measured with an accuracy of better than  $1 \text{ \AA/sec}$ . Dual electron beams with dual targets may be used to coevaporate composite materials in E-beam evaporation systems.

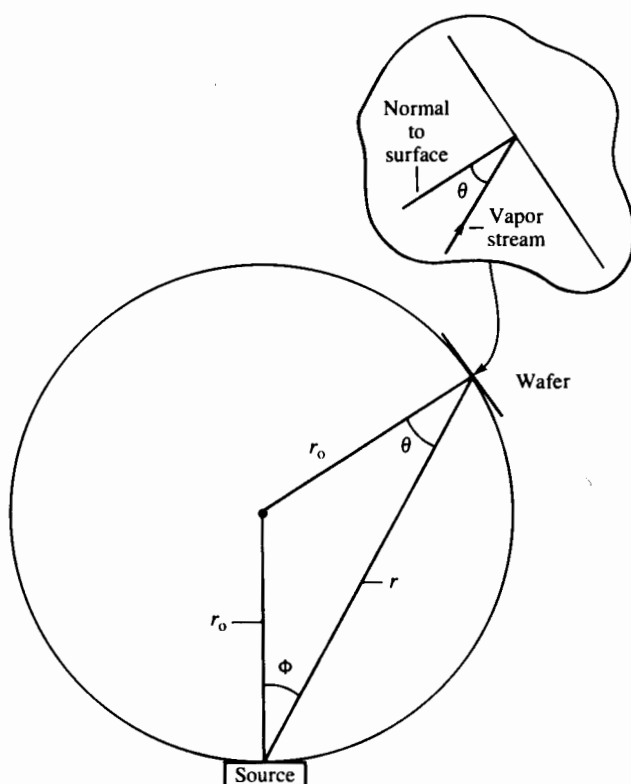
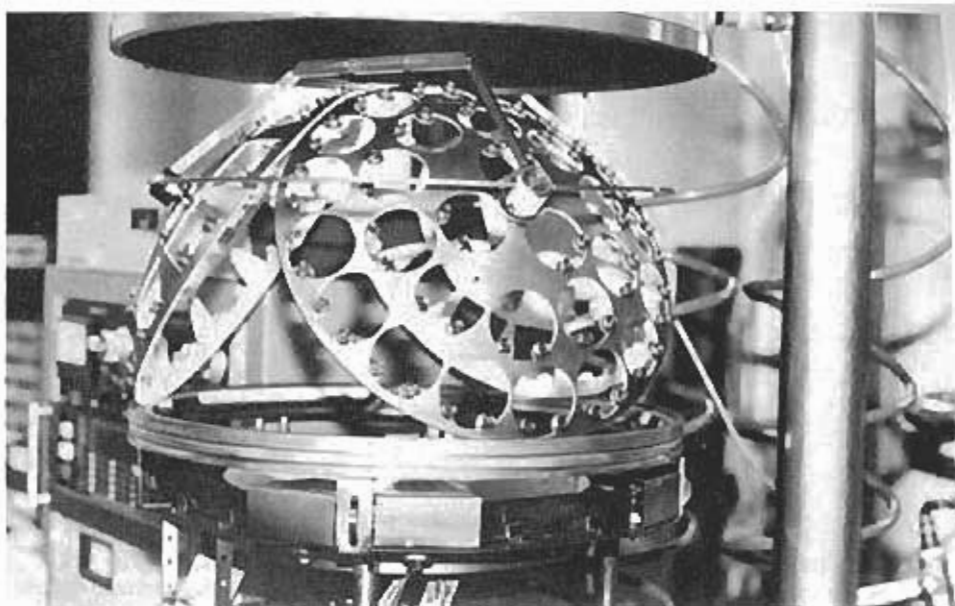


Fig. 6.3 Geometry for evaporation in a system using a planetary substrate holder.

X-ray radiation can be generated in an electron-beam system for acceleration voltages exceeding 5 to 10 keV. Substrates may suffer some radiation damage from both energetic electrons and X-rays. The damage can usually be annealed out during subsequent process steps. However, the radiation effects are of great concern to MOS process designers, and so sputtering has replaced electron-beam evaporation in many steps in manufacturing processes.

### 6.1.4 Flash Evaporation

Flash evaporation uses a fine wire as the source material, and a high-temperature ceramic bar is used to evaporate the wire. The wire is fed continuously and evaporates on contact with the ceramic bar. Flash evaporation can produce relatively thick films, as in an E-beam system, without problems associated with radiation damage.



**Fig. 6.4** Photograph of an E-beam evaporation system with a planetary substrate holder which rotates simultaneously around two axes.

### 6.1.5 Shadowing and Step Coverage

Because of the large mean free paths of gas molecules at low pressure, evaporation techniques tend to be directional in nature, and shadowing of patterns and poor step coverage can occur during deposition. Figure 6.5 illustrates the shadowing phenomenon which can occur with closely spaced features on the surface of an integrated circuit. In the fully shadowed region, there will be little deposition. In the partially shadowed region, there will be variation in film thickness. To minimize these effects, the planetary substrate holder of the electron-beam system continuously rotates the wafers during the film deposition.

## 6.2 SPUTTERING

Sputtering is achieved by bombarding a target with energetic ions, typically  $\text{Ar}^+$ . Atoms at the surface of the target are knocked loose and transported to the substrate, where deposition occurs. Electrically conductive materials such as Al, W, and Ti can use a dc power source, in which the target acts as the cathode in a diode system. Sputtering of dielectrics such as silicon dioxide or aluminum oxide requires an RF power source to supply energy to the argon atoms. A diagram of a sputtering system is shown in Fig. 6.6.

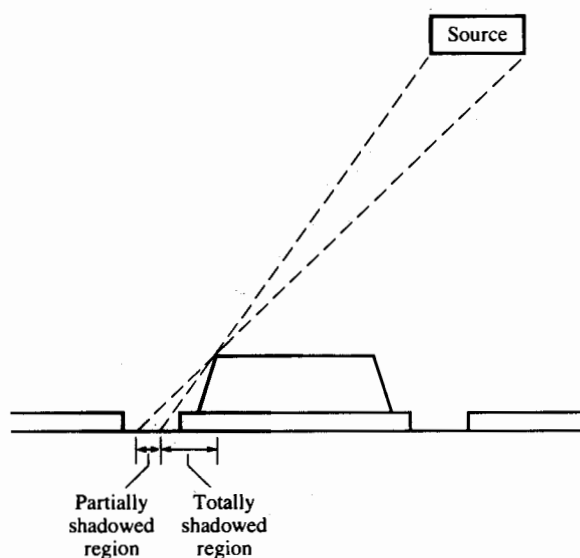


**Fig. 6.5** An example of the shadowing problem that can occur in low-pressure vacuum deposition in which the molecular mean free path is large.

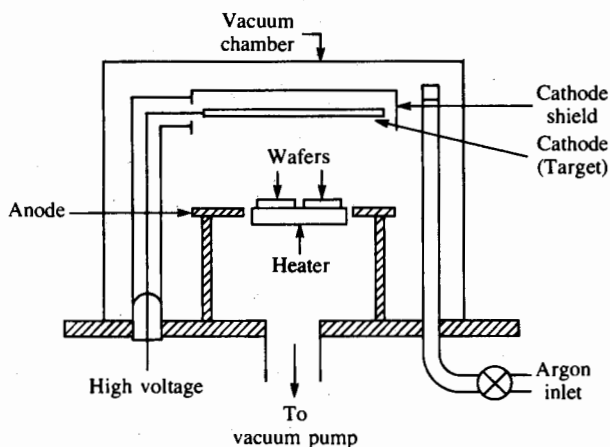


**Fig. 6.6** A dc sputtering system in which the target material acts as the cathode of a diode and the wafers are mounted on the system anode.

In sputter deposition, there is a threshold energy which must be exceeded before sputtering occurs. The sputtering yield (Fig. 6.7) is the ratio of the number of atoms liberated from the target by each incident atom, and it increases rapidly with energy of the incident atoms. Systems are usually operated with an energy large enough to ensure a sputtering yield of at least unity.



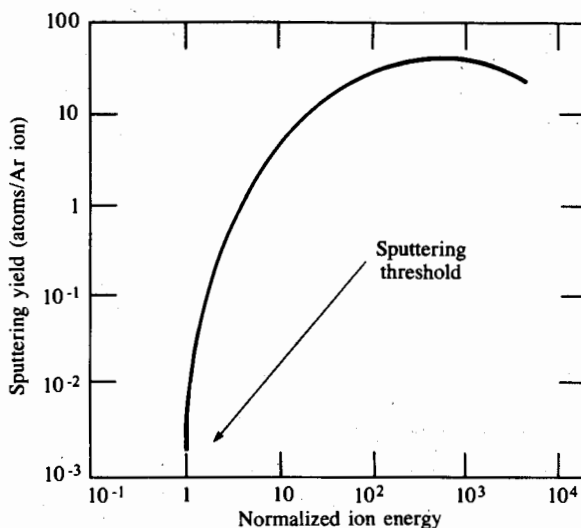


Fig. 6.7 Sputtering yield versus ion energy for a dc sputtering system using argon.

Sputtering can be used to deposit a broad range of materials. In addition, alloys may be deposited in which the film has the same composition as the target. An example is the Al-Cu-Si alloy commonly used for metallization in integrated circuits. (We will discuss this alloy in Chapter 7.) As one might expect, sputtering results in the incorporation of some argon into the film, and heating of the substrate up to 350 °C can occur during the deposition process. Sputtering can also give excellent coverage of the sharp topologies often encountered in integrated circuits.

Sputter etching (a reversal of the sputter deposition process) can be used to clean the substrate prior to film deposition, and the sputter etching process is often used to clean contact windows prior to metal deposition. Etching removes any residual oxide from the window and improves the contact between the metal and the underlying material.

### 6.3 CHEMICAL VAPOR DEPOSITION

Chemical vapor deposition (CVD) forms thin films on the surface of a substrate by thermal decomposition and/or reaction of gaseous compounds. The desired material is deposited directly from the gas phase onto the surface of the substrate. Polysilicon, silicon dioxide, and silicon nitride are routinely deposited using CVD techniques. In addition, refractory metals such as tungsten (W) can also be deposited using CVD.

Chemical vapor deposition can be performed at pressures for which the mean free path for gas molecules is quite small, and the use of relatively high temperatures can result in excellent conformal step coverage over a broad range of topological profiles.

### 6.3.1 CVD Reactors

Several different types of CVD reactor systems are shown in Fig. 6.8. In Fig. 6.8a, a continuous atmospheric-pressure reactor is shown. This type of reactor is often used for deposition of the silicon dioxide passivation layer as one of the last steps in integrated-circuit processing. The reactant gases flow through the center section of the reactor and are contained by nitrogen curtains at the ends. The substrates can be fed continuously through the system, and large-diameter wafers are easily handled. However, high gas-flow rates are required by the atmospheric-pressure reactor.

The hot-wall, low-pressure system of Fig. 6.8b is commonly used to deposit polysilicon, silicon dioxide, and silicon nitride, and is referred to as an LPCVD (low-pressure CVD) system. The reactant gases are introduced into one end of a three-zone furnace tube and are pumped out the other end. Temperatures range from 300 to 1150 °C, and the pressure is typically 30 to 250 Pa. Excellent uniformity can be obtained with LPCVD systems, and several hundred wafers may be processed in a single run. Hot-wall systems have the disadvantage that the deposited film simultaneously coats the inside of the tube. The tube must be periodically cleaned or replaced to minimize problems with particulate matter. In spite of this problem, hot-wall LPCVD systems are in widespread use throughout the semiconductor industry.

CVD reactions can also take place in a plasma reactor, as shown in Fig. 6.8c. Formation of the plasma permits the reaction to take place at low temperatures, which is a primary advantage of plasma-enhanced CVD (PECVD) processes. In the parallel-plate system, the wafers lie on a grounded aluminum plate which serves as the bottom electrode for establishing the plasma. The wafers can be heated up to 400 °C using high-intensity lamps or resistance heaters. The top electrode is a second aluminum plate placed in close proximity to the wafer surface. Gases are introduced along the outside of the system, flow radially across the wafers, and are pumped through an exhaust in the center. An RF signal is applied to the top plate to establish the plasma. The capacity of this type of system is limited, and wafers must be loaded manually. A major problem in VLSI fabrication is particulate matter that may fall from the upper plate onto the wafers.

The furnace-plasma system in Fig. 6.8d can handle a large number of wafers at one time. A special electrode assembly holds the wafers parallel to the gas flow. The plasma is established between alternating groups of electrodes supporting the wafers.

### 6.3.2 Polysilicon Deposition

Silicon is deposited in an LPCVD system using thermal decomposition of silane:



Low-pressure systems (25 to 150 Pa) use either 100% silane or 20 to 30% silane diluted with nitrogen. A temperature between 600 and 650 °C results in deposition of polysilicon material at a rate of 100 to 200 Å/min. A less commonly used deposition occurs between

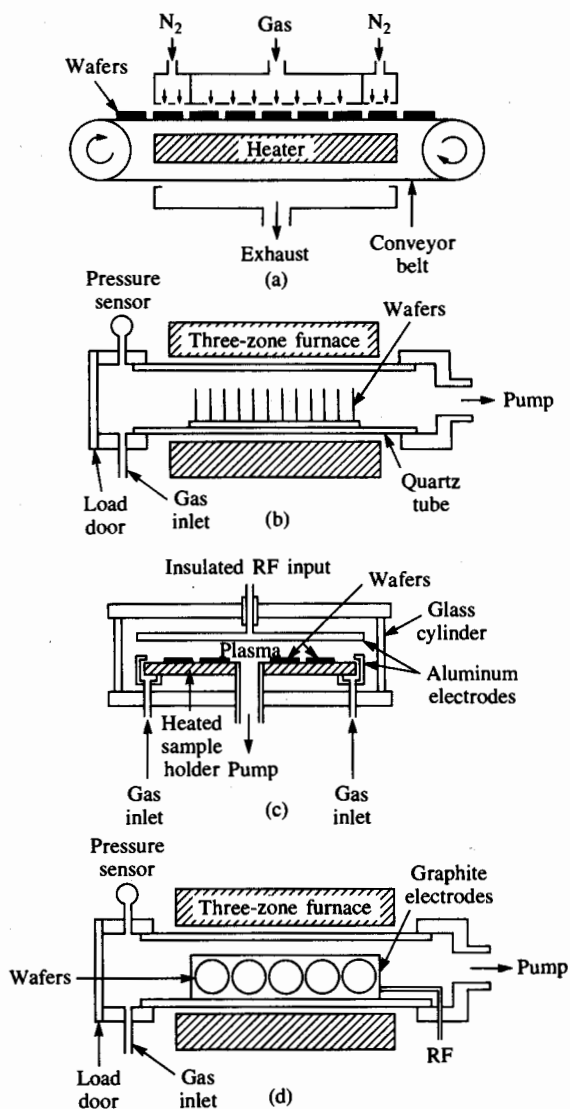


**Fig. 6.8** Four types of chemical vapor deposition (CVD) systems. (a) Atmospheric-pressure reactor; (b) hot-wall LPCVD system using a three-zone furnace tube; (c) parallel-plate plasma-enhanced CVD system; (d) PECVD system using a three-zone furnace tube. Copyright, 1983, Bell Telephone Laboratories, Inc. Reprinted by permission from ref. [2].

850 and 1050 °C in a hydrogen atmosphere. The higher temperature overcomes a reduction in deposition rate caused by the hydrogen carrier gas.

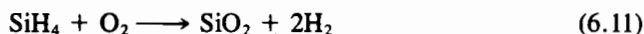
Polysilicon can be doped by diffusion or ion implantation or during deposition (in situ) by the addition of dopant gases such as phosphine, arsine, or diborane. The addition of diborane greatly increases the deposition rate, whereas the addition of phosphine or arsine substantially reduces the deposition rate.

Polysilicon is often deposited as undoped material and is then doped by diffusion. High-temperature diffusion occurs much more rapidly in polysilicon than in single-crystal silicon, and the polysilicon film is typically saturated with the dopant to achieve as low a resistivity as possible for interconnection purposes. Resistivities of 0.01 to 0.001 ohm-cm can be achieved in diffusion-doped polysilicon. Ion implantation typically yields a lower active-impurity density in the polysilicon film, and ion-implanted polysilicon exhibits a resistivity about ten times higher than that achieved by high-temperature diffusion.

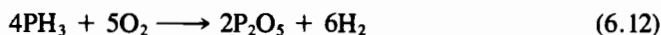
### 6.3.3 Silicon Dioxide Deposition

Silicon dioxide films can be deposited using a variety of reactions and temperature ranges, and the films can be doped or undoped. Phosphorus-doped oxide can be used as a passivation layer over a completed integrated circuit or as the insulating medium in multilevel metal processes (which will be discussed in the next chapter). Silicon dioxide containing 6 to 8% phosphorus by weight will soften and flow at temperatures between 1000 and 1100 °C. This "P-glass reflow" process is often used to improve step coverage and provide a smoother topography for later process steps. SiO<sub>2</sub> with lower concentrations of phosphorus will not reflow properly, and higher concentrations can corrode aluminum if moisture is present. Oxide doped with 5 to 15% by weight of various dopants can also be used as a diffusion source.

Deposition of silicon dioxide over aluminum must occur at a temperature below the silicon-aluminum eutectic point of 577 °C (see Chapter 7). A reaction between silane and oxygen is commonly used between 300 and 500 °C:



The oxide may be doped with phosphorus using phosphine:



Oxide passivation layers can be deposited at atmospheric pressure using the continuous reactor of Fig. 6.8a, or they can be deposited at reduced pressure in an LPCVD system, as in Fig. 6.8b.

Deposition of SiO<sub>2</sub> films prior to metallization can be performed at higher temperatures, which gives a wider choice of reactions and results in better uniformity and step coverage. For example, a dichlorosilane reaction with nitrous oxide in an LPCVD

system at approximately 900 °C,



is used to deposit insulating layers of  $\text{SiO}_2$  on wafer surfaces.

Decomposition of the vapor produced from a liquid source, *tetraethylorthosilicate* (TEOS), can also be used in an LPCVD system between 650 and 750 °C.



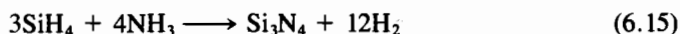
Deposition based on the decomposition of TEOS provides excellent uniformity and step coverage. Oxide doping may be accomplished in the LPCVD systems by adding phosphine, arsine, or diborane.

A comparison of some of the properties of various CVD oxides is given in Table 6.1.

### 6.3.4 Silicon Nitride Deposition

As discussed in Chapter 3, silicon nitride is used as an oxidation mask in recessed oxide processes. Silicon nitride is also used as a final passivation layer because it provides an excellent barrier to both moisture and sodium contamination. Composite films of oxide and nitride are being investigated for use as very thin gate insulators in scaled VLSI devices, and they are also used as the gate dielectric in electrically programmable memory devices.

Both silane and dichlorosilane will react with ammonia to produce silicon nitride. The silane reaction occurs between 700 and 900 °C at atmospheric pressure:



Dichlorosilane is used in an LPCVD system between 700 and 800 °C:

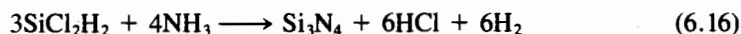
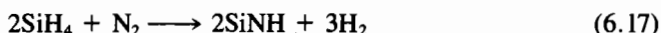


**Table 6.1** Properties of Various Deposited Oxides. (After ref. [2].)

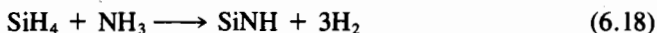
Source	Deposition Temperature (°C)	Composition	Conformal Step Coverage	Dielectric Strength (MV/cm)	Etch Rate (Å/min) [100:1 H <sub>2</sub> O:HF]
Silane	450	SiO <sub>2</sub> (H)	No	8	60
Dichlorosilane	900	SiO <sub>2</sub> (Cl)	Yes	10	30
TEOS	700	SiO <sub>2</sub>	Yes	10	30
Plasma	200	SiO <sub>1.9</sub> (H)	No	5	400

Thermal growth of silicon nitride is also possible but not very practical. Silicon nitride will form when silicon is exposed to ammonia at temperatures between 1000 and 1100 °C, but the growth rate is very low.

Plasma systems may also be used for the deposition of silicon nitride. Silane will react with a nitrogen discharge to form plasma nitride (SiN):



Silane will also react with ammonia in an argon plasma:



LPCVD films are hydrogen-rich, containing up to 8% hydrogen. Plasma deposition does not produce stoichiometric silicon nitride films. Instead, the films contain as much as 20 to 25% hydrogen. LPCVD films have high internal tensile stresses, and films thicker than 2000 Å may crack because of this stress. On the other hand, plasma-deposited films have much lower tensile stresses.

The resistivity ( $10^{16}$  ohm-cm) and dielectric strength (10 MV/cm) of the LPCVD nitride film are better than those of most plasma films. Resistivity of plasma nitride can range from  $10^6$  to  $10^{15}$  ohm-cm, depending on the amount of nitrogen in the film, while the dielectric strength ranges between 1 and 5 MV/cm.

### 6.3.5 CVD Metal Deposition

Many metals can be deposited by CVD processes. Molybdenum (Mo), tantalum (Ta), titanium (Ti), and tungsten (W) are all of interest in today's processes because of their low resistivity and their ability to form silicides with silicon (see Chapter 7). Aluminum can be deposited from a metallorganic compound such as tri-isobutyl aluminum, but this technique has not been commonly used because many other excellent methods of aluminum deposition are available.

Tungsten can be deposited by thermal, plasma, or optically assisted decomposition of  $\text{WF}_6$ :



or through reduction with hydrogen:



Mo, Ta, and Ti can be deposited in an LPCVD system through reaction with hydrogen. The reaction is the same for all three metals:



where M stands for any one of the three metals mentioned above.

## 6.4 EPITAXY

Chemical vapor deposition processes can be used to deposit silicon onto the surface of a silicon wafer. Under appropriate conditions, the silicon wafer acts as a seed crystal, and a single-crystal silicon layer is grown on the surface of the wafer. The growth of a crystalline silicon layer from the vapor phase is called *vapor-phase epitaxy* (VPE), and it is the most common form of epitaxy used in silicon processing. In addition, *liquid-phase epitaxy* (LPE) and *molecular-beam epitaxy* (MBE) are being used widely in GaAs technology.

Epitaxial growth was first used in integrated-circuit processing to grow single-crystal  $n$ -type layers on  $p$ -type substrates for use in standard buried-collector bipolar processing. More recently, it has been introduced into CMOS VLSI processes where lightly doped layers are grown on heavily doped substrates of the same type ( $n$  on  $n^+$  or  $p$  on  $p^+$ ) to help suppress a circuit-failure mode called *latchup*.

### 6.4.1 Vapor-Phase Epitaxy

Silicon epitaxial layers are commonly grown with silicon deposited from the gas phase. A basic model for the process is given in Fig. 6.9. At the silicon surface, the flux  $J_s$  of gas molecules is determined by

$$J_s = k_s N_s \quad (6.22)$$

in which  $k_s$  is the surface-reaction rate constant and  $N_s$  is the surface concentration of the molecule involved in the reaction. In the steady state, this flux must equal the flux  $J_g$  of molecules diffusing in from the gas stream. The flux  $J_g$  may be approximated by

$$J_g = (\bar{D}_g/\delta)(N_g - N_s) = h_g(N_g - N_s) \quad (6.23)$$

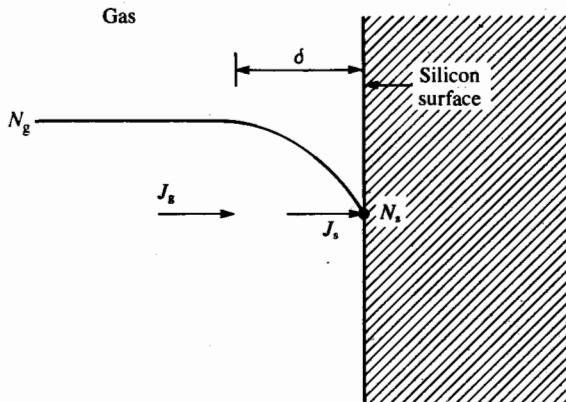


Fig. 6.9 Schematic model for the epitaxial growth process.

in which  $\bar{D}_g$  is an effective diffusion constant for the gas molecule and  $\delta$  is the distance over which the diffusion is taking place. The ratio  $\bar{D}_g/\delta$  is called the *vapor-phase mass-transfer coefficient*,  $h_g$ . Equating  $J_s$  and  $J_g$  yields the flux impinging on the surface of the wafer. The growth rate is equal to the flux divided by the number  $N$  of molecules incorporated per unit volume of film.

$$v = \frac{J_s}{N} = \frac{k_s h_g}{k_s + h_g} \frac{N_g}{N} \quad (6.24)$$

If  $k_s \gg h_g$ , then growth is said to be mass-transfer-limited, and

$$v = h_g \frac{N_g}{N} \quad (6.25)$$

If  $h_g \gg k_s$ , then growth is said to be surface-reaction-limited, and

$$v = k_s \frac{N_g}{N} \quad (6.26)$$

Figure 6.10 shows epitaxial growth rate as a function of temperature. Chemical reactions at the surface tend to follow an Arrhenius relationship characterized by an activation

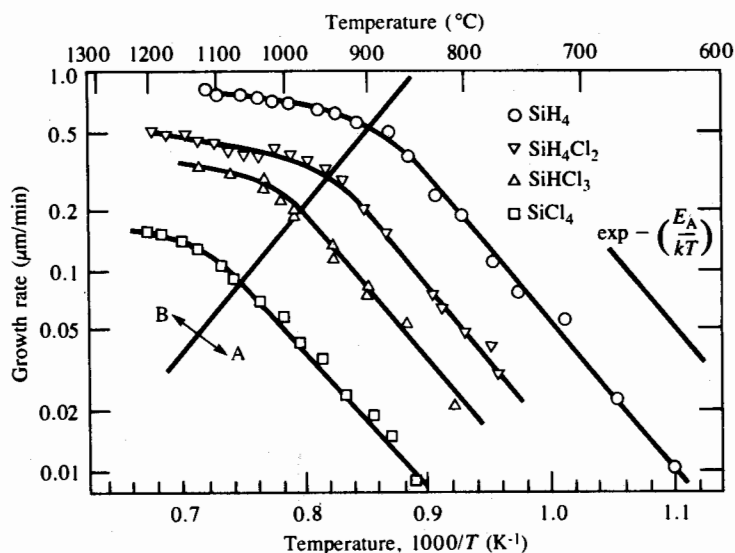


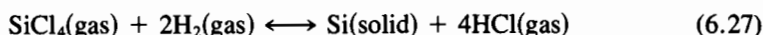
**Fig. 6.10** Temperature dependence of the silicon epitaxial growth process for four different sources. The growth rate is surface-reaction-limited in region A and is mass-transfer-limited in region B. Reprinted with permission from Philips Journal of Research from ref. [3].



energy  $E_A$ , whereas the mass-transfer process tends to be independent of temperature. These two regions show up clearly in this figure. At low temperatures, the growth rate follows an Arrhenius relationship with an activation energy of approximately 1.5 eV. At higher temperatures, the growth rate becomes independent of temperature. In order to have good growth-rate control and to minimize sensitivity to variations in temperature, epitaxial growth conditions are usually chosen to yield a mass-transfer-limited growth rate.

Three common types of VPE reactors, the horizontal, vertical, and barrel systems, are shown in Fig. 6.11. The susceptor that supports the wafers is made of graphite and is heated by RF induction in the horizontal and vertical reactors and by radiant heating in the barrel reactor.

Silicon tetrachloride ( $\text{SiCl}_4$ ), silane ( $\text{SiH}_4$ ), dichlorosilane ( $\text{SiH}_2\text{Cl}_2$ ), and trichlorosilane ( $\text{SiHCl}_3$ ) have all been used for silicon VPE. Silicon tetrachloride has been widely used in industrial processing:



This reaction takes place at approximately 1200 °C and is reversible. If the carrier gas coming into the reactor contains hydrochloric acid, etching of the surface of the silicon wafer can occur. This in situ etching process can be used to clean the wafer prior to the start of epitaxial deposition.

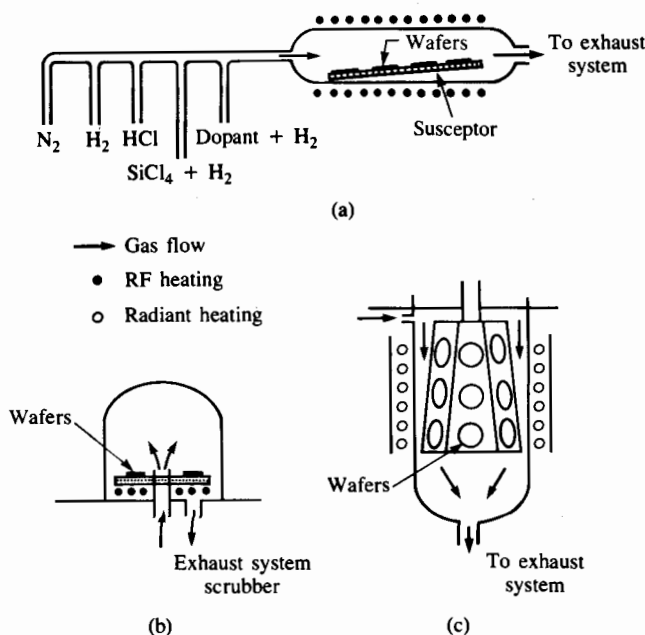


**Fig. 6.11** (a) Horizontal, (b) pancake, and (c) barrel susceptors commonly used for vapor-phase epitaxy. Copyright, 1985, John Wiley & Sons, Inc., with permission from ref. [1].

A second reaction competes with the epitaxial deposition process:



This second reaction also etches the silicon from the wafer surface. If the concentration of  $\text{SiCl}_4$  is too high, etching of the wafer surface will take place rather than epitaxial deposition. Figure 6.12 shows the effect of  $\text{SiCl}_4$  concentration on the growth of epitaxial silicon. The growth rate initially increases with increasing  $\text{SiCl}_4$  concentration, peaks, then decreases. Eventually, growth stops and the etching process becomes dominant. If the growth rate is too high, a polysilicon layer is deposited rather than a layer of single-crystal silicon.

Epitaxial growth can also be achieved by the pyrolytic decomposition of silane:



The reaction is not reversible and takes place at low temperatures. In addition, it avoids the formation of  $\text{HCl}$  gas as a reaction by-product. However, careful control of the reactor is needed to prevent formation of polysilicon rather than single-crystal silicon layers. The presence of any oxidizing species in the reactor can also lead to contamination of the epitaxial layer by silica dust.

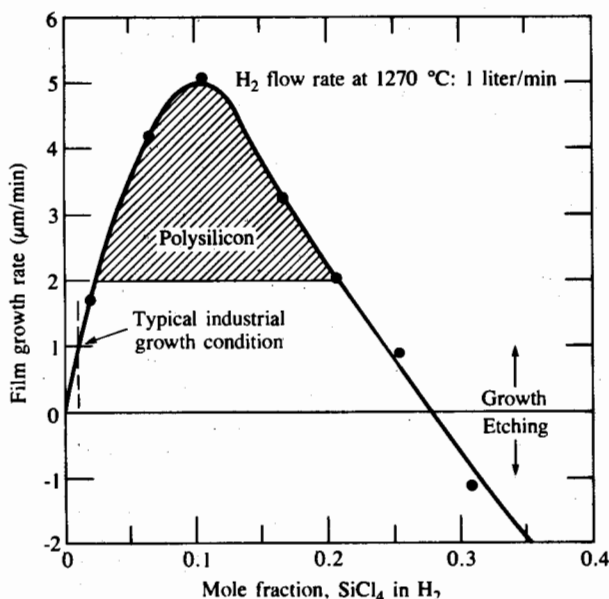


**Fig. 6.12** Silicon epitaxial growth rate as a function of  $\text{SiCl}_4$  concentration. Polysilicon deposition occurs for growth rates exceeding 2  $\mu\text{m}/\text{min}$ . Etching of the surface will occur for mole fraction concentrations exceeding 28%. Copyright, 1985, John Wiley & Sons, Inc., with permission from ref. [1].

### 6.4.2 Doping of Epitaxial Layers

Epitaxial layers may be doped during the growth process by adding impurities to the gas used for deposition. Arsine, diborane, and phosphine are the most convenient sources of the common impurities. The resistivity of the epitaxial layer is controlled by varying the partial pressure of the dopant species in the gas supplied to the reactor. The addition of arsine or phosphine tends to slow down the rate of epitaxial growth, while the addition of diborane tends to enhance the epitaxial growth rate.

Lightly doped epitaxial layers are often grown on more heavily doped substrates, and "autodoping" of the epitaxial layer can occur during growth. Impurities can evaporate from the wafer or may be liberated by chlorine etching of the surface during deposition. The impurities are incorporated into the gas stream, resulting in doping of the growing layer. As the epitaxial layer grows, less dopant is released from the wafer into the gas stream, and the impurity profile eventually reaches a constant level determined by the doping in the gas stream.

During deposition, the substrate also acts as a source of impurities which diffuse into the epitaxial layer. This "out-diffusion" will be discussed more fully in the next section. Both autodoping and out-diffusion cause the transition from the doping level of the substrate to that of the epitaxial layer to be less abrupt than desired. The effects of autodoping and out-diffusion are illustrated in Fig. 6.13.

### 6.4.3 Buried Layers

Out-diffusion is a common problem that occurs with the buried layer in bipolar transistors. In order to reduce the resistance in series with the collector of the bipolar transistor, heavily doped  $n$ -type regions are diffused into the substrate prior to the growth of an  $n$ -type epitaxial layer. During epitaxy, impurities diffuse upward from the heavily doped buried-layer regions.

Diffusion of impurities from the substrate during epitaxial growth is modeled by the diffusion equation with a moving boundary,<sup>[4]</sup> as in Fig. 6.14:

$$D \frac{\partial^2 N}{\partial x^2} = \frac{\partial N}{\partial t} + v_x \frac{\partial N}{\partial x} \quad (6.30)$$

in which  $v_x$  is the rate of growth of the epitaxial layer.

Two specific solutions of eq. (6.30) are applicable to epitaxial layer growth. The first case is the growth of an undoped epitaxial layer on a uniformly doped substrate. The boundary conditions are  $N(x, 0) = N_s = N(\infty, t)$ , and the flux  $J_x = (h + v_x)N(0, t)$  where  $h$  is the mass-transfer coefficient which characterizes the escape rate of dopant atoms from the silicon into the gas. Normally,  $h \ll v_x$ . A change of variables from  $x$  to  $x' = x - v_x t$  simplifies eq. (6.30) and gives an approximate solution for  $N(x, t)$ :

$$N_1(x, t) = \frac{N_s}{2} \left[ 1 + \operatorname{erfc} \frac{x - x_{\text{epi}}}{2\sqrt{D_s t}} \right] \quad (6.31)$$

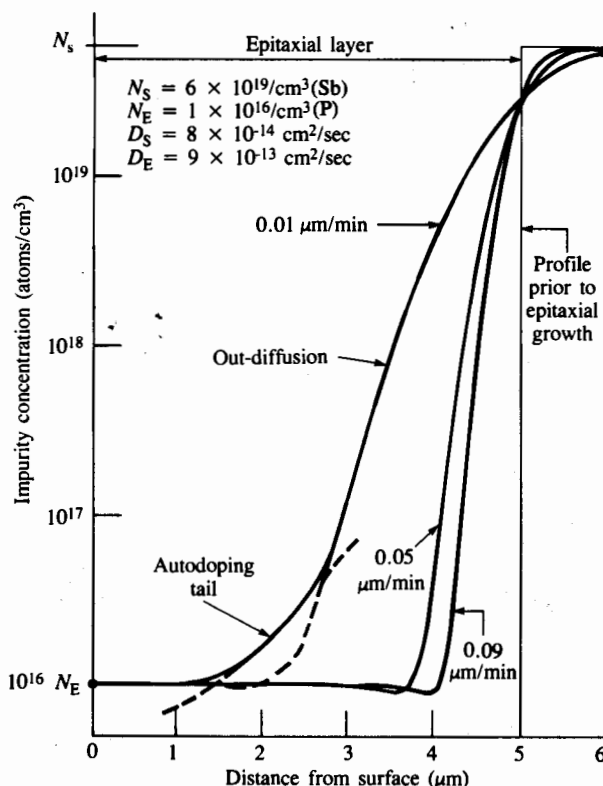


**Fig. 6.13** Redistribution of impurity atoms due to gas-phase autodoping and impurity out-diffusion during epitaxial layer growth. Out-diffusion is calculated using eq. (6.33) for epitaxial growth of a phosphorus-doped layer at 1150 °C over an antimony-doped buried layer with a surface concentration of  $6 \times 10^{19}/\text{cm}^3$ . The three curves are for growth rates of 0.01, 0.05, and 0.09  $\mu\text{m}/\text{min}$ . For clarity, the effects of autodoping are shown on only one curve.

Eq. (6.31) assumes that the epitaxial layer growth rate greatly exceeds the rate of movement of the diffusion front. Eq. (6.31) is the exact solution for diffusion from one semi-infinite layer into a second semi-infinite layer.

The second case is the growth of a doped epitaxial layer on an undoped substrate. The boundary conditions for this case are  $N(0, t) = N_E$ , and  $N(\infty, t) = 0 = N(x, 0)$ . The solution of eq. (6.30) for these boundary conditions is:

$$N_2(x, t) = \frac{N_E}{2} \left[ \operatorname{erfc} \frac{x - x_{\text{epi}}}{2\sqrt{D_E t}} + \exp \frac{v_x x}{D_E} \operatorname{erfc} \frac{x + x_{\text{epi}}}{2\sqrt{D_E t}} \right] \quad (6.32)$$

in which  $x_{\text{epi}} = v_x t$  is the epitaxial layer thickness. Superposition of the solutions for

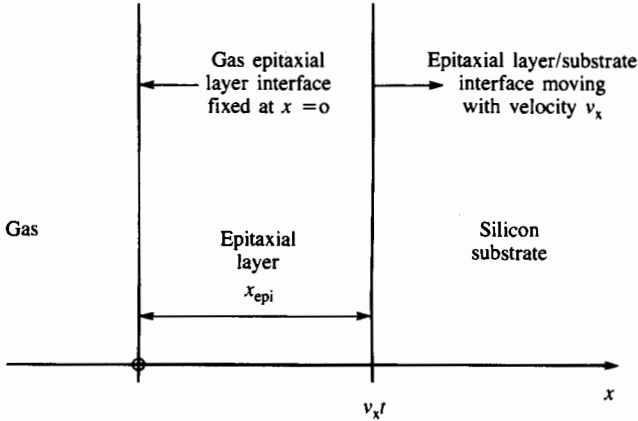


Fig. 6.14 Geometrical structure of moving boundary value problem which models the epitaxial growth process.

these two cases gives a good approximation to diffusion which occurs during epitaxial growth:

$$N(x, t) = N_1(x, t) + N_2(x, t) \quad (6.33)$$

$N_s$  represents the doping in the substrate, and  $N_E$  is the doping intentionally introduced into the epitaxial layer.  $D_s$  and  $D_E$  represent the diffusion coefficients of the impurity species in the substrate and epitaxial layer, respectively. Figure 6.13 shows diffusion profiles for a phosphorus-doped epitaxial layer grown at various rates on an antimony-doped substrate. The curves were produced using eq. (6.33).

An additional problem occurs during epitaxial growth. The oxidation and lithographic processing steps used during formation of a buried layer result in a step of as much as  $0.2 \mu\text{m}$  around the perimeter of the buried layer. Epitaxial growth on this nonplanar surface causes the pattern to shift during growth, as illustrated in Fig. 6.15. Pattern shift is difficult to predict, may be as large as the epitaxial layer thickness, and must be accounted for during the design of subsequent mask levels.

#### 6.4.4 Liquid-Phase and Molecular-Beam Epitaxy

In liquid-phase epitaxy, the substrate is brought into contact with a solution containing the material to be deposited in liquid form. The substrate acts as a seed for material crystallizing directly from the solute. Growth rates typically range between  $0.1$  and  $1 \mu\text{m}/\text{min}$ .

In the molecular-beam epitaxy process, the crystalline layer is formed by deposition from a thermal beam of atoms or molecules. Deposition is performed in ultrahigh-

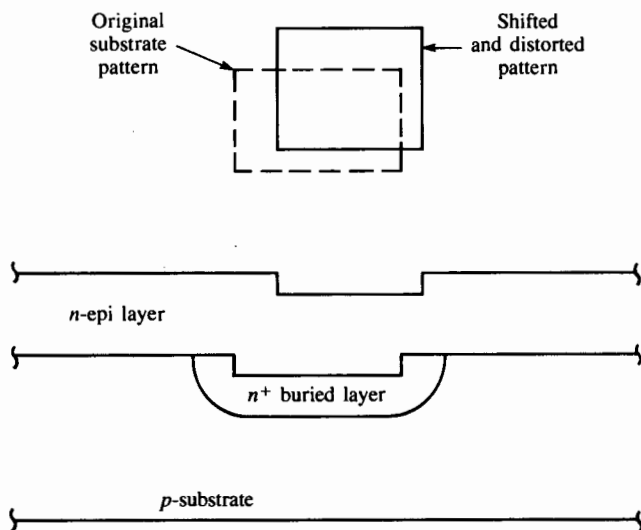


**Fig. 6.15** Pattern shift during epitaxial growth over an  $n^+$  buried layer. The original pattern is shifted and distorted in shape.

vacuum conditions ( $10^{-8}$  Pa). Substrate temperatures during MBE range from 400 to 900 °C, and the growth rate is relatively low (0.001 to 0.3  $\mu\text{m}/\text{min}$ ). The epitaxial layer is grown atomic layer by atomic layer, and many unique device structures can be fabricated by changing the material which is deposited between one layer and the next.

The throughput of MBE is relatively low at the present time. Plasma-assisted CVD processes, which promise to give many of the benefits of MBE with much higher throughput, are presently being investigated in research laboratories.

## 6.5 SUMMARY

Thin films of a very broad range of materials are used in integrated-circuit fabrication. This chapter has presented an overview of film-deposition techniques including physical evaporation, chemical vapor deposition (CVD), epitaxial growth, and sputtering. Most of these processes are performed at low pressure, and this chapter has presented an introduction to vacuum systems and a review of some important aspects of ideal gas theory.

Physical evaporation using filament or electron-beam evaporators can be used to deposit metals and other materials which can easily be melted. E-beam systems can operate at high power levels and melt high-temperature metals. However, E-beam evaporation may result in radiation damage to thin oxide layers at the surface of the wafer. In addition, it is difficult to deposit material compounds and alloys using evaporation. Finally, gas molecules at low pressures have large mean free paths, and evaporation has problems with shadowing and poor step coverage during film deposition.

Sputtering uses energetic ions such as argon to bombard a target material and dislodge atoms from the surface of the target. The dislodged atoms are deposited on the surface of the wafer. Direct-current sputtering systems can be used to deposit conductive materials, and RF sputtering can be used to deposit insulators. Sputtering can be used to deposit composite materials in which the deposited film maintains the same composition as the source material. Sputtering also uses higher pressures than evaporation. The much shorter mean free paths which result yield a deposition with freedom from shadowing and much better step coverage.

Low-pressure and atmospheric chemical vapor deposition (CVD) systems deposit films from chemical reactions taking place in a gas stream passing over the wafer. Polysilicon, silicon dioxide, silicon nitride, and metals can all be deposited using CVD techniques. A special type of CVD deposition called epitaxy results in the growth of single-crystal silicon films on the surface of silicon wafers. Out-diffusion and autodoping cause problems with impurity profile control during epitaxial layer growth.

In a modern bipolar or MOS fabrication process, one can expect to find evaporation, sputtering, and chemical vapor deposition techniques all used somewhere in the process flow.

## REFERENCES

- [1] S. M. Sze, *Semiconductor Devices — Physics and Technology*, John Wiley & Sons, New York, 1985.
- [2] A. C. Adams, "Dielectric and Polysilicon Film Deposition," Chapter 3 in S. M. Sze, Ed., *VLSI Technology*, McGraw-Hill, New York, 1983.
- [3] F. C. Eversteyn, "Chemical-Reaction Engineering in Semiconductor Industry," *Philips Research Reports*, 29, 45–66 (February, 1974).
- [4] A. B. Glaser and G. E. Subak-Sharpe, *Integrated Circuit Engineering*, p. 205–209, Addison-Wesley, Reading, MA, 1979.
- [5] W. S. Ruska, *Microelectronic Processing*, McGraw-Hill, New York, 1987.

## FURTHER READING

1. J. L. Vossen and W. Kern, Eds., *Thin Film Processes*, Academic Press, New York, 1978.
2. J. F. O'Hanlon, *A User's Guide to Vacuum Technology*, John Wiley & Sons, New York, 1980.
3. L. Holland, *Vacuum Deposition of Thin Films*, John Wiley & Sons, New York, 1961.
4. A. S. Grove, *Physics and Technology of Semiconductor Devices*, John Wiley & Sons, New York, 1967.
5. H. C. Theuerer, "Epitaxial Silicon Films by Hydrogen Reduction of  $\text{SiCl}_4$ ," *Journal of the Electrochemical Society*, 108, 649–653 (July, 1961).
6. C. O. Thomas, D. Kahng, and R. C. Manz, "Impurity Distribution in Epitaxial Silicon Films," *Journal of the Electrochemical Society*, 109, 1055–1061 (November, 1962).

7. A. S. Grove, A. Roder, and C. T. Sah, "Impurity Distribution in Epitaxial Growth," *Journal of Applied Physics*, **36**, 802–810 (March, 1965).
8. D. Kahng, C. O. Thomas, and R. C. Manz, "Epitaxial Silicon Junctions," *Journal of the Electrochemical Society*, **110**, 394–400 (May, 1963).
9. W. H. Shepherd, "Vapor Phase Deposition and Etching of Silicon," *Journal of the Electrochemical Society*, **112**, 988–994 (October, 1965).
10. G. R. Srinivasan, "Autodoping Effects in Silicon Epitaxy," *Journal of the Electrochemical Society*, **127**, 1334–1342 (June, 1980).
11. J. C. Bean, "Silicon Molecular Beam Epitaxy as a VLSI Processing Technique," 1981 IEEE IEDM Proceedings, p. 6–13.

## PROBLEMS

- 6.1 A silicon wafer sits on a bench in the laboratory at a temperature of 300 K and a pressure of 1 atm. Assume that the air consists of 100% oxygen. How long does it take to deposit one atomic layer of oxygen on the wafer surface, assuming 100% adhesion?
- 6.2 Calculate the impingement rate and mean free path for oxygen molecules ( $M = 32$ ) at 300 K and a pressure of  $10^{-4}$  Pa. What is this pressure in torr?
- 6.3 An ultrahigh vacuum system operates at a pressure of  $10^{-8}$  Pa. What is the concentration of residual air molecules in the chamber at 300 K?
- 6.4 The partial pressure of a material being deposited in a vacuum system must be well above the residual background gas pressure if reasonable deposition rates are to be achieved. What must the partial pressure of aluminum be to achieve a deposition rate of 100 nm/min? Assume close packing of spheres with a diameter of 5 Å, and 100% adhesion of the impinging aluminum.
- 6.5 A wafer 100 mm in diameter is mounted in an electron-beam evaporation system in which the spherical radius is 40 cm. Use eq. (6.7) to estimate the worst-case variation in film thickness between the center and edges of the wafer for an evaporated aluminum film 1  $\mu\text{m}$  thick.
- 6.6 A MBE system must operate under ultrahigh vacuum conditions to prevent the formation of undesired atomic layers on the surface of the substrate. What pressure is required if formation of a monolayer of contamination can be permitted after the sample has been in the chamber for no less than 4 hr?
- 6.7 (a) Calculate the growth rate of a silicon layer from a  $\text{SiCl}_4$  source at 1200 °C. Use  $h_g = 1$  cm/sec,  $k_s = 2 \times 10^6 \exp(-1.9/kT)$  cm/sec, and  $N_g = 3 \times 10^{16}$  atoms/cm<sup>3</sup>. (For silicon,  $N = 5 \times 10^{22}$ /cm<sup>3</sup>.)  
 (b) What is the change in growth rate if the temperature is increased by 25 °C?  
 (c) At what temperature does  $k_s = h_g$ ? What is the growth rate at this temperature?  
 (d) What is the value of  $E_A$  in Fig. 6.8?
- 6.8 Use eqs. (6.31) and (6.32) to model the case of a 10- $\mu\text{m}$   $n$ -type epitaxial layer ( $N_E = 1 \times 10^{16}$ /cm<sup>3</sup>) grown on a  $p$ -type substrate ( $N_S = 1 \times 10^{18}$ /cm<sup>3</sup>). Plot the impurity profile



in the epitaxial layer and substrate assuming that the layer was grown at a rate of  $0.2 \mu\text{m}/\text{min}$  at a temperature of  $1200^\circ\text{C}$ . Assume boron and phosphorus are the impurities. Find the location of the  $pn$  junction.

**6.9** Compare and discuss the advantages and disadvantages of evaporation, sputtering, and chemical vapor deposition.

**6.10** A 1-kg source of aluminum is used in an E-beam evaporation system. How many 100-mm wafers can be coated with a  $1\text{-}\mu\text{m}$  Al film before the source material is exhausted? Assume that 15% of the evaporated aluminum actually coats a wafer. (The rest is deposited on the inside of the electron-beam system.)

**6.11** A silicon wafer 75 mm in diameter is centered 100 mm above a small planar evaporation source. Calculate the ratio of thickness between the center and edges of the wafer using eq. (6.7), following a  $1\text{-}\mu\text{m}$  film deposition.